ELSEVIER

Thermochimica Acta 280/281 (1996) 279–287

thermochimica acta

Kinetics of the primary, eutectic and polymorphic crystallization of metallic glasses studied by continuous scan methods [1]

I. Telleria [a,*], J. M. Barandiarán [b]

[a] *Departamento de Física de Materiales, Universidad del Pais Vasco/EHU. Apdo. 1072, 20080 San Sebastian, Spain*

[b] *Departamento de Electricidad y Electrónica, Universidad del Pais Vasco/EHU. Apdo. 644, 48080 Bilbao, Spain*

Abstract

The crystallization kinetics of glassy $Co_{78}Si_{13}B_9$ (primary), $Pd_{80}Si_{20}$, $Fe_{80}B_{20}$ (eutectic) and $Co_{75}B_{25}$ (polymorphic) have been studied with differential scanning calorimetry and analysed with non-isothermal theoretical expressions. The analysis gives good agreement with isothermal studies in the polymorphic case and in the eutectic $Fe_{80}B_{20}$, with accurate values of the activation energy and Avrami index. Two superimposed peaks, related to surface and bulk nucleation, have been found in the eutectic alloy $Pd_{80}Si_{20}$. Although the separation of the parameters of each peak is very difficult, the second one can be fitted to a non-isothermal equation, with activation energy very close to the isothermal values reported in the literature. A better fit of the observed behaviour is found using a Vogel–Fulcher rate constant in this alloy. The primary crystallization is driven by diffusion processes, and does not fit the Avrami equations. This results in long tails of the non-isothermal peaks which cannot be analysed accurately with the usual methods. The kinetic parameters of all the alloys change with temperature, indicating that, even when a good fit is obtained, the usual expressions for non-isothermal analysis are only valid in narrow ranges.

Keywords: $Co_{75}B_{25}$; $Co_{78}Si_{13}B_9$; Crystallization kinetics; DSC; Eutectic crystallization; $Fe_{80}B_{20}$; Metallic glasses; $Pd_{80}Si_{20}$; Polymorphic crystallization; Primary crystallization

* Corresponding author.

[1] Dedicated to Professor Hiroshi Suga.

SSDI 0040-6031(95)02648-7

1. Introduction

Crystallization of metallic glasses is a process of great interest both from a fundamental point of view and concerning possible applications. In particular, for magnetic applications, heat treatment in order to relax quenched-in stresses and to induce some kind of magnetic anisotropy is systematically performed on these materials. The starting of crystallization during such treatments is to be avoided in order to maintain the excellent magnetic properties of the amorphous state. Very recently nanocrystalline materials, obtained by controlled grain growth of a crystalline phase in a metallic glass, have been used, both to obtain permanent magnets and to obtain very soft magnetic materials. This has renewed the interest of the study of crystallization kinetics.

Differential scanning calorimetry is a common tool in the study of crystallization of metallic glasses. It gives a curve of the rate of enthalpy release, as a function of the temperature, during heating at a constant rate. This procedure is easy and convenient from the experimental point of view, but the analysis of the non-isothermal curves is difficult. It is usually performed on the basis of the well known Johnson–Mehl–Avrami equation, which is isothermally deduced from the assumption of nucleation and growth process. In some cases, however this assumption can be too simplistic, and long-range diffusion or other mechanisms can be involved. In fact three kinds of crystallization can occur for metallic glasses, namely primary, eutectic and polymorphic; each is expected to behave in a different way. The analysis is particularly difficult when several processes are involved in the same peak.

In this work we present the non-isothermal treatment of three different kinds of glass whose crystallization covers all the possible kinds of transformation process: primary ($Co_{78}Si_{13}B_9$), eutectic ($Pd_{80}Si_{20}$ and $Fe_{80}B_{20}$) and polymorphic ($Co_{75}B_{25}$). The different kinetic equations available to the analysis are discussed, and the kinetic parameters obtained are compared with the isothermal values found in the literature.

2. Experimental

The experimental curves were obtained with a Perkin–Elmer DSC-4 with computerized data acquisition system, the temperatures in the instrument were calibrated from the melting of pure Zn and K_2SO_4. Specimens of mass 2–4 mg were heated at constant heating rates between 1 and 80 K min^{-1} in gold containers under a pure nitrogen atmosphere. Samples were continuously heated at 160 K min^{-1} from room temperature to 100 K below the onset temperature of crystallization, to reduce annealing effects.

3. Crystallization under continuous scan conditions

The crystallization kinetics of amorphous alloys [1] are typical of those of a solid–solid reaction. If the rate at which the crystallized fraction α grows can be

expressed as

$$\frac{d\alpha}{dt} = [K(T)]f(\alpha) \tag{1}$$

where $K(T)$ is the rate constant and $f(\alpha)$ is the function which reflects the mechanism of crystallization, we can integrate under non-isothermal conditions. In particular for a constant heating rate $R = dT/dt$, one obtains:

$$\int_0^{\alpha} \frac{d\alpha}{f(\alpha)} = \frac{1}{R}\int_{T_i}^{T} K(T)dT \tag{2}$$

This results in an $\alpha(T)$ curve whose derivative can be compared directly with the DSC peaks.

The most frequently used expressions for $f(\alpha)$ are:

(1) For a Johnson–Mehl–Avrami (JMA) equation

$$f(\alpha) = n(1-\alpha)\{\ln[1/(1-\alpha)]\}^{(n-1)/n} \tag{3a}$$

where n represents both nucleation rate and growth morphology;

(2) For transformations with parabolic growth laws, such as those involving long-range diffusion:

$$f(\alpha) = m(1-\alpha)\alpha^{(m-1)/m} \tag{3b}$$

where the values of m are 3/2 or 5/2.

On the other hand, although the rate constant $K(T)$ depends on a number of parameters, viscosity is the most important factor in the temperature range at which crystallization occurs, then $K(T) \cong C/\eta(T)$, and two cases can be envisaged:

(1) With an Arrhenius expression for the viscosity, the rate constant $K(T)$ becomes:

$$K(T) \cong K_0 \exp(E/k_B T) \tag{4a}$$

where K_0 and E are the pre-exponential factor and the activation energy for the process;

(2) With a Vogel–Fulcher expression, $K(T)$ becomes:

$$K(T) \cong K_0 \exp\{1/[b(T-T_0)]\} \tag{4b}$$

where b and T_0 are empirical parameters which have been physically interpreted only in the framework of the free volume theory.

The combination of a JMA mechanism and an Arrhenius rate constant has been widely used. Introducing Eqs. (3a) and (4a) into Eq. (2) gives:

$$\alpha \cong 1 - \exp\left\{-\left[\frac{K_0 k_B T^2}{R E}\left(1 - \frac{2k_B T}{E}\right)\exp\left(-\frac{E}{k_B T}\right)\right]^n\right\} \tag{5}$$

and differentiating with respect to temperature, we obtain:

$$\frac{d\alpha}{dT} = \frac{nK_0}{R}\exp\left(-\frac{E}{k_B T}\right)\exp\left[-\left(\frac{S}{R}\right)^n\right]\left(\frac{S}{R}\right)^{(n-1)} \tag{6}$$

with

$$S = \frac{K_0 k_B T^2}{E}\left(1 - 2\frac{k_B T}{E}\right)\exp\left(-\frac{E}{k_B T}\right)$$

Eq. (5) can be applied at the temperature, T_p, at which $d\alpha/dT$ is maximum. At this temperature, $\alpha(T_p)$ is a constant ($\alpha(T_p) \cong 0.62$) independent of the heating rate. By so doing we obtain the Kissinger equation:

$$\ln\frac{T_p^2}{R} = \frac{E}{k_B T_p} + \ln\frac{K_0 k_B}{E} \tag{7}$$

after some algebra.

If a Vogel–Fulcher rate constant is used together with the JMA expression for $f(\alpha)$, a modified expression of the form:

$$\ln\frac{(T_p - T_0)^2}{R} = \frac{1}{b(T_p - T_0)} - \ln[1 - 2b(T_p - T_0)] + \ln K_0 b \tag{8}$$

can be deduced [2].

In any case, by fitting the experimental T_p values at different heating rates R to these equations we can obtain the parameters for the rate constant, e.g. activation energies or T_0, and pre-exponential factors. The Avrami index, or other information concerning the crystallization mechanism, can be deduced from the fitting of the whole peak to the non-isothermal expression, Eq. (6), or to an equivalent one.

4. Results and discussion

Fig. 1 shows the experimental DSC curves, normalized for sample weight, indicating the peaks which were analysed.

The Kissinger plots of $\ln R/T_p^2$ vs $1/T_p$ are shown in Fig. 2. The values obtained for the activation energy and preexponential factor, compared with earlier results reported in the literature for isothermal experiments, are given in Table 1. Excellent agreement is obtained in all cases.

In the figure, the results obtained with the sample $Pd_{80}Si_{20}$ show a curvature that may indicate a Vogel–Fulcher rate constant. Parameters of Eq. (4b) for such a rate constant were obtained by fitting the experimental points to Eq. (8) following the method described in Ref. [2]. We obtained the values $K_0 = 6 \times 10^6\,s^{-1}$ $b = 2 \times 10^{-4}\,K^{-1}$ and $T_0 = 428\,K$, which are more likely to represent the true behaviour of the viscosity. In particular the values of b and T_0 can be compared with those obtained directly from the viscosity in Ref. [10] and show very good agreement.

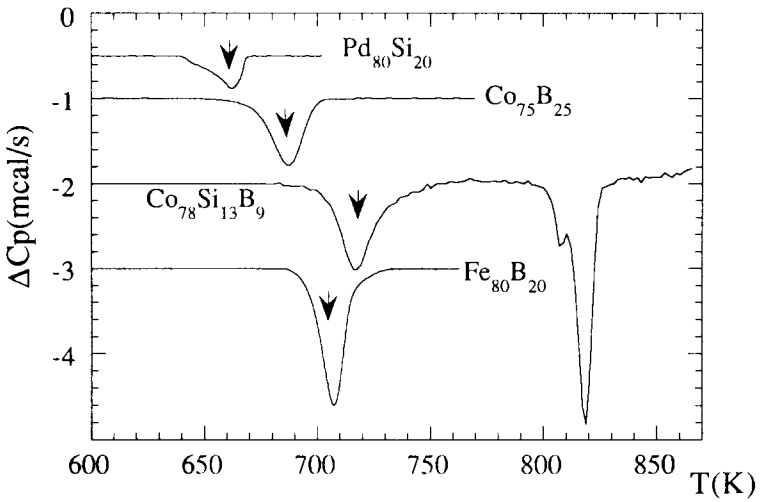

Fig. 1. DSC peaks of the studied samples, indicating those analysed in this work.

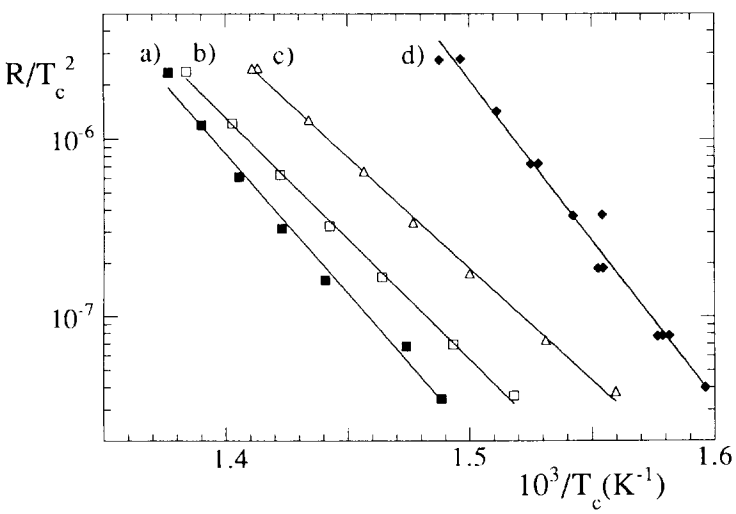

Fig. 2. Kissinger plot for the samples: (a) $Co_{78}Si_{13}B_9$, (b) $Fe_{80}B_{20}$, (c) $Co_{75}B_{25}$, (d) $Pd_{80}Si_{20}$.

Table 1
Values of kinetic parameters obtained for the samples studied

Sample	K_0/s^{-1}	E/eV	Refs.
$Co_{78}Si_{13}B_9$	4×10^{19}	3.1	
$Co_{75}B_{25}$	1×10^{16}	2.5	2.3 eV; Ref. [3]
$Pd_{80}Si_{20}$	1.5×10^{25}	3.6	3.1–3.8 eV; Refs. [4]–[6]
$Fe_{80}B_{20}$	1×10^{17}	2.7	2.1–2.7 eV; Refs. [7]–[9]

The measured experimental values of $d\alpha/dt$ were fitted to Eq. (6) for all the rates and samples with the values of K_0 and E obtained with the Kissinger method. Fig. 3 shows this fitting for the crystallization peaks at $R = 5°C\,min^{-1}$.

Depending on the crystallization reaction in each sample we obtain different results:

(1) When the crystallization of the sample is primary ($Co_{78}Si_{13}B_9$), the experimental data do not fit at temperatures higher than T_p. In this case, a better fit is obtained by considering $f(\alpha)$ as a parabolic law with $m = 5/2$. In this way, Eq. (2), numerically integrated, fits the data down to the half height in the high temperature side (Fig. 3a).

(2) When crystallization is eutectic, the results of the fitting are much better than in the preceding result. This is the case for $Fe_{80}B_{20}$ where only a small number of very low relative intensity points are not fitted in the extreme high temperature side of the crystallization peak (Fig. 3b).

On the other hand, the crystallization peak of $Pd_{80}Si_{20}$ shows clearly two different processes at low heating rates—a shoulder appears on the low temperature part of the crystallization peak. At high heating rates, however, the two processes are mixed up and it is almost impossible to separate them.

This particular alloy was extensively studied by Kelton and Spaepen [11] some years ago, and they concluded that a surface nucleation process takes place at the first stages of crystallization. The surface nucleation sites are rapidly exhausted, and the crystallization proceeds afterwards by homogeneous nucleation and growth in the bulk of the sample. This behaviour has been confirmed by other authors also [4].

In order to take into account the existence of these two processes, the last part of the peak, including the peak maximum, were fitted to Eq. (6) and the values of E, K_0 and n deduced for the bulk crystallization. The theoretical peak for this process was then subtracted and the surface crystallization could be analysed. This latter process gave an activation energy of $E = 2.9\,eV$ and preexponential factor K_0 of about $5 \times 10^{20}\,s^{-1}$. A simultaneous fitting to the two processes is shown in Fig. 3c.

It must be noticed that the fit has always been performed by using Arrhenius expressions for the rate constant. This is not a source of inaccuracy because the variation of the apparent activation energy, given by a Vogel–Fulcher constant, is very small in the temperature range of a single peak. The extremely high values of $K_0(10^{20}$–$10^{25}\,s^{-1})$, however, indicate the actual behaviour of the viscosity is a Vogel–Fulcher one.

(3) When the crystallization is polymorphic ($Co_{75}B_{25}$) very good fitting is obtained over all the crystallization peak (Fig. 3d).

The kinetic parameters E, K_0 and n do not take single values for any sample. It appears that E or K_0 change, together with n, if they are left free to vary in order to get the best fit for each peak. In this way, activation energy increases or preexponential factor decreases with increasing temperature for all the samples, but changes are not very systematic. In order to obtain more systematic results we kept a fixed activation energy and concentrate on the variation of K_0 and n. Fig. 4 shows the variation of K_0 as

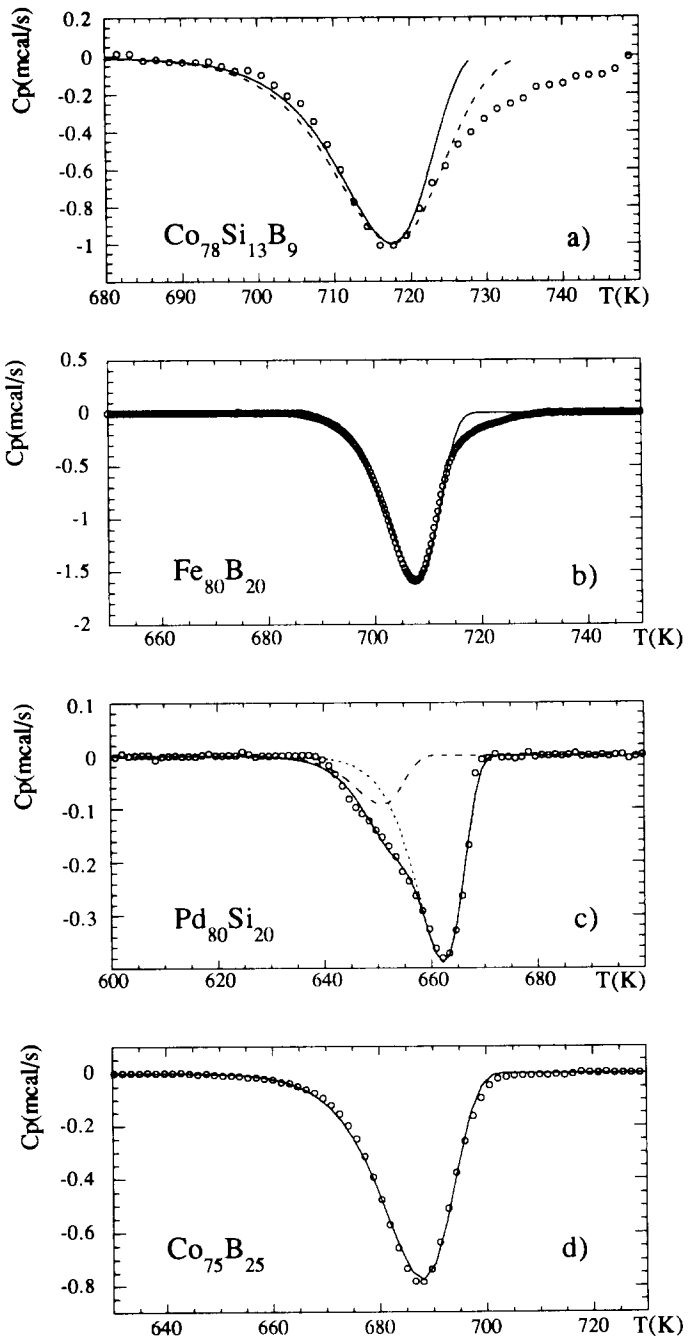

Fig. 3. Experimental DSC crystallization data (○) for all samples studied at 5 K min^{-1}. Calculated curves corresponding to Eq. (6) are shown by full lines.

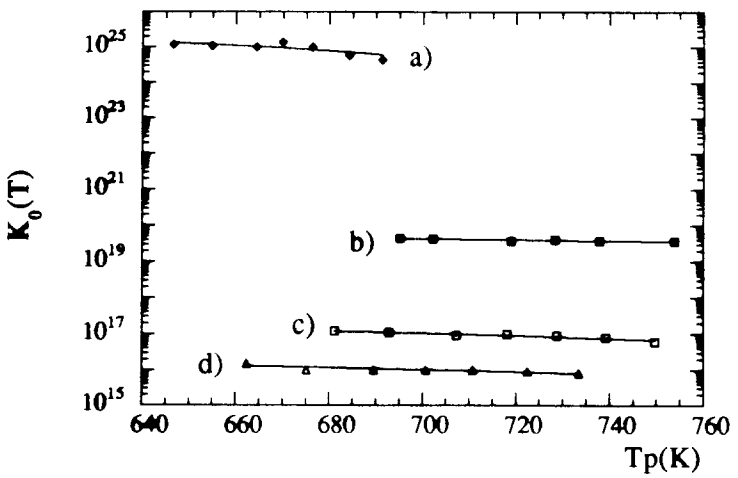

Fig. 4. Variation of the preexponential factor of all the samples studied as a function of T_p: (a) $Pd_{80}Si_{20}$, (b) $Co_{78}Si_{13}B_9$, (c) $Fe_{80}B_{20}$, (d) $Co_{75}B_{25}$.

a function of the temperature of the maximum of the crystallization peak T_p. A slight decrease is observed in all cases. This variation is not surprising taking into account that the Arrhenius behaviour of the viscosity is modulated by several temperature-dependent factors in order to get the rate constant $K(T)$.

Fig. 5 shows the evolution of the Avrami index as a function of the peak temperature T_p. Two different trends are observed. $Pd_{80}Si_{20}$ and $Co_{78}Si_{13}B_9$ show rather constant

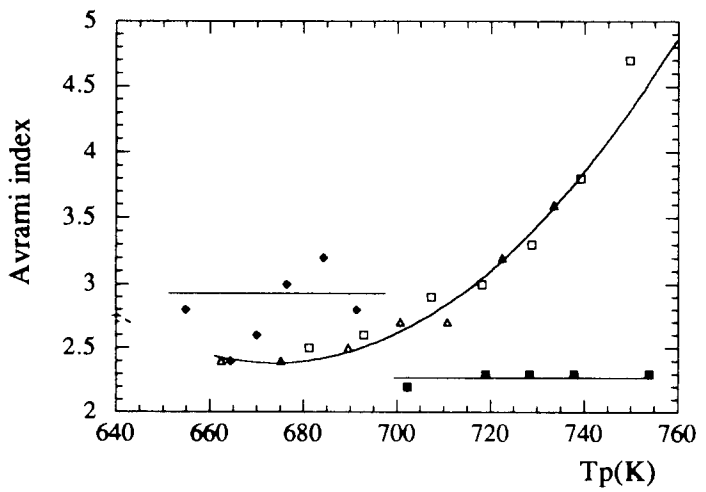

Fig. 5. Variation of Avrami index of all the samples studied as a function of T_p: ◆ $Pd_{80}Si_{20}$, △ $Co_{75}B_{25}$, □ $Fe_{80}B_{20}$, ■ $Co_{78}Si_{13}B_9$.

values of n in all the temperature ranges studied. In the former sample only the bulk crystallization has been studied, and some "noise" is always present as a consequence of the mixing of the surface crystallization process. In the other two samples the increase of n with temperature is exactly the same, reaching very high and unrealistic values at high temperatures. Similar behaviour has been reported from isothermal measurements in Fe–B- and Fe–Ni-based amorphous samples [12, 13]. This change could be related to the different behaviour of the nucleation rate which evolves during the crystallization. At low temperatures heterogeneous nucleation is more likely to take place, whereas at high temperature homogeneous nucleation, or even a increasing rate nucleation can drive the transformation.

In any case, Avrami indices higher than five are not theoretically expected, although they have been reported on several occasions [12, 14, 15]. This can indicate that, even when a good fit is obtained, the usual expressions for non-isothermal analysis are only valid in narrow ranges, and processes changing with temperature usually take place at the crystallization of metallic glasses. Isothermal measurements do not present such high variations because very high transformation rates avoid any isothermal measurement at high temperatures.

References

[1] J.W. Christian, The Theory of Transformations in Metals and Alloys, 2nd edn., Pergamon Press, 1975.
[2] I. Tellería and J.M. Barandiarán in A. Conde, C.F. Conde and M. Millan (Eds.), Trends in Non-Crystalline Solids, World Scientific, Singapore, 1992, p. 181.
[3] U. Koster and U. Herold, in H.-J. Guntherodt and H. Beck (Eds.) Glassy Metals I: Topics in Applied Physics, Vol. 46, Springer, 1981, p. 225.
[4] T. Spassov, Cryst. Res. Technol., 27 (1992) 149.
[5] P. Duhaj, D. Barancok and A. Ondrejka, J. Non-Cryst. Solids, 21 (1976) 411.
[6] M.A. Marcus, J. Non-Cryst. Solids, 30 (1979) 317.
[7] L.A. Davis, R. Ray, C.-P. Chou and R.C. O'Handley, Sc. Metall., 10 (1976) 541.
[8] F.E. Luborsky, Mater. Sci. Eng., 28 (1977) 139.
[9] J.A. Leake and A.L. Greer, J. Non-Cryst. Solids, 38/39 (1980) 735.
[10] H.S. Chen and G. Goldstein, J. Appl. Phys., 43 (1972) 1642.
[11] K.F. Kelton and F. Spaepen, Acta Metall., 33 (1985) 455.
[12] T. Kemény, I. Vincze and B. Fogarassy, Phys. Rev. B: 20 (1979) 476.
[13] M.G. Scott, J. Mater. Sci., 13 (1978) 291.
[14] E. Coleman, Mater. Sci. Eng., 23 (1976) 161.
[15] G. Vlasák, P. Duhaj, V. Svajlenová and P. Svec, J. Non-Cryst. Solids, 99 (1988) 65.